Soria-Verdugo, A., Morato-Godino, A., Garcia-Gutierrez, L. M. & Garcia-Hernando, N. (2017). Pyrolysis of sewage sludge in a fixed and a bubbling fluidized bed – Estimation and experimental validation of the pyrolysis time. *Energy Conversion and Management*, vol. 144, pp. 235–242.

DOI: 10.1016/j.enconman.2017.04.062

Pyrolysis of sewage sludge in a fixed and a bubbling fluidized bed – Estimation and experimental validation of the pyrolysis time

Antonio Soria-Verdugo*, Andres Morato-Godino, Luis Miguel Garcia-Gutierrez, Nestor Garcia-Hernando

Carlos III University of Madrid (Spain), Energy Systems Engineering Group, Thermal and Fluids Engineering Department. Avda. de la Universidad 30, 28911 Leganés (Madrid, Spain).

** corresponding author: asoria@ing.uc3m.es*

Abstract

Pyrolysis of sewage sludge was studied experimentally in a stainless-steel reactor operated as a fixed or fluidized bed. A novel measuring technique, consisting of measuring the mass of the whole reactor and the sample on a scale, was applied. The scale was capable of measuring the whole mass of the reactor with enough accuracy to detect the mass released by the sewage sludge sample during its pyrolysis. This original measuring technique permitted the measurement of the evolution over time of the mass of sewage sludge supplied to the bed in batch during its pyrolysis while moving freely in the bed. From the measurement of the mass of the solid residue remaining in the reactor, the pyrolysis time of the sewage sludge sample can be obtained accurately for each operating condition. Different operating conditions were selected to analyze the evolution with time of the sample mass during the pyrolysis process, including the bed temperature and the velocity of the Nitrogen used as inert gas. An increase of the velocity of Nitrogen from that of a

fixed bed ($0.8U_{mf}$) to that of a low velocity bubbling fluidized bed ($2.5U_{mf}$) accelerates remarkably the pyrolysis process, i.e. reduces the pyrolysis time, however increasing the Nitrogen velocity further has a slight effect on the characteristic velocity of the pyrolysis process. The pyrolysis process of sewage sludge can also be accelerated by increasing the bed temperature, even though the effect of the temperature is lower than that of the Nitrogen velocity. Furthermore, a mathematical model based on a first order apparent kinetics for the pyrolysis of sewage sludge was proposed. The model was employed to estimate the pyrolysis time for each operating condition, obtaining a proper agreement with the experimental measurements.

Keywords: Sewage sludge; pyrolysis; fixed bed; fluidized bed; pyrolysis time.

Notation

d_{bm} Particle diameter of the bed material [m].

d_i Inner diameter of the reactor [m].

d_p Particle diameter of sewage sludge [m].

g Gravity acceleration [m s^{-2}]

h Height of the reactor [m].

h_b Height of the fixed bed [m].

k Apparent rate constant [s^{-1}].

k_{500} Apparent rate constant for a reactor temperature of 500 ºC [s^{-1}].

k_{600} Apparent rate constant for a reactor temperature of 600 ºC [s^{-1}].

45 m Mass of the sample [kg].

46 m_0 Initial mass of the sample [kg].

47 m_{vol} Mass of volatiles remaining in the sample [kg].

48 m_{vol0} Initial mass of volatiles in the sample [kg].

49 m_{res} Mass of the solid residue in the sample [kg].

50 n Reaction order [-].

51 t Time [s].

52 t_{mod} Estimated pyrolysis time [s].

53 t_{pyr} Experimental pyrolysis time [s].

54 T Temperature [K].

55 T_{amb} Reference temperature [K].

56 U Gas velocity [m s^{-1}].

57 U_{mf} Minimum fluidization velocity [m s^{-1}].

58 V/V* Reacted fraction [%].

59 X Percentage of mass of the sample [%].

60 X_{vol} Percentage of total volatile content [%].

61 X_{res} Percentage of solid residue [%].

62 ε_t Relative error of the pyrolysis time [%].

63 ε Void fraction of the bed material [-].

ρ_{bm} Particle density of the bed material [kg m^{-3}].

ρ_g Gas density at reactor temperature [kg m^{-3}].

$\rho_{g,amb}$ Gas density at reference temperature [kg m^{-3}].

μ_g Gas dynamic viscosity at reactor temperature [kg m^{-1} s^{-1}].

$\mu_{g,amb}$ Gas dynamic viscosity at reference temperature [kg m^{-1} s^{-1}].

ϕ Sphericity of the dense phase particles [-].

1. Introduction

Sewage sludge is the solid residue produced during the treatment of municipal and industrial wastewater. The rapid development of urbanization and industrialization has contributed to the dramatic increase of sewage sludge production over the last decades [1], causing a critical problem of waste management. The ways of disposing sewage sludge can be divided into three main applications: landfill, agricultural use, and incineration or thermochemical conversion [2]. Nonetheless, the European regulations limit the use of sewage sludge for landfilling due to environmental problems, while the use for agricultural purposes has been also restricted because of the harmful components of sewage sludge such as heavy metals, polyaromatic hydrocarbons, and polychlorinated biphenyls [3]. In contrast, sewage sludge thermochemical conversion permits to recover energy, reduces the volume of the residue by 70% and thermally destructs the pathogens [4].

Among the different thermochemical conversion processes, pyrolysis is considered to be a promising sewage sludge disposal technology due to its

advantages, such as residue volume reduction, concentration of heavy metals, and stabilization of waste [5]. Pyrolysis processes can be divided into conventional or fast pyrolysis, depending mainly on the pyrolysis vapors residence time in the reactor. In conventional pyrolysis, vapor residence times can vary between 5 and 30 min, whereas in fast pyrolysis processes, typical vapor residence times are around 1-5 s [6]. Fast pyrolysis of biomass is usually employed for fuel liquid production because of the high yield of bio-oil generated [7]. Even though fast pyrolysis of biomass has achieved a commercial status [8], many aspects are still empirical, requiring further study to improve the efficiency and reliability of the process, and the final product characteristics [9].

Despite the numerous studies published focusing on thermochemical conversion of sewage sludge, most of them work with dry sludge due to the significant reduction of the efficiency and the operating problems derived from the conversion of wet sewage sludge. In this way, fluidized bed reactors permit both the thermochemical conversion and the drying processes to be carried out in the same reactor, avoiding a significant decrease in efficiency. Fluidized beds are employed as industrial chemical reactors due to their ability to convert low quality solid fuels, even wet sewage sludge, with a high efficiency and with an associated low emission of pollutants. The homogeneous and low reaction temperature of fluidized beds limits the emissions of NO_x, whereas sorbent bed materials can be used for in-bed capture of SO_x emissions. The technology of bubbling fluidized beds is adequate for the conversion of highly volatile fuels such as biomass and organic waste, for which the conversion can occur in the bubbling bed at low temperatures without the need of in-bed heat exchangers [10]. The performance and emission level of bubbling fluidized beds are

111 influenced by fuel mixing [11], which can be improved by increasing the
112 fluidizing gas velocity [12-15].

113 The products obtained from the pyrolysis of biomass in a fluidized bed are
114 affected by the operating conditions, such as fuel particle diameter, pyrolysis
115 vapors residence time and reactor temperature. The bed temperature is
116 considered to be the most influential parameter and thus several authors have
117 focused their research on analyzing its effect on the liquid yield [16-18]. In these
118 works, the bed temperature that maximizes the liquid yield is studied. For low
119 reactor temperatures, the energy supplied to the fuel particles is limited and
120 thus the total amount of volatile matter is not released from the solid fuel. In
121 contrast, for high reactor temperatures, the pyrolysis vapors generated may
122 suffer secondary cracking reactions, resulting in an increase of non-
123 condensable gases, decreasing the liquid yield. Therefore, the optimal reactor
124 temperature to produce liquid fuel from a pyrolysis process is a moderate
125 temperature. Concerning the maximum bio-oil yield produced from the pyrolysis
126 of sewage sludge in fluidized bed reactors, Jaramillo-Arango et al. [19] obtained
127 a liquid production of 40 wt% for a temperature of 600 °C; the maximum liquid
128 yield reached by Alvarez et al. [20] was 48 wt% for a bed temperature of 500
129 °C; and Fonts et al. [21] reached a maximum liquid production of 40 wt% at a
130 temperature of 550 °C. Sun et al. [22] studied the pyrolysis of sewage sludge in
131 a wide range of temperatures between 300 and 900 ºC, concluding that the
132 maximum liquid production from the condensation of the pyrolysis vapors was
133 obtained at moderate temperatures of around 550 ºC. In fact, in a following
134 study [5], they focused the analysis of sewage sludge pyrolysis on a narrow
135 temperature range of 400-600 ºC. Moreover, for temperatures above 650 ºC the

char generated during the pyrolysis process may react with the water vapor produced [23].

The secondary thermal cracking of the pyrolysis vapors depends also on their residence time inside the reactor. To avoid the thermal cracking of the product gas, which promotes the formation of non-condensable gases and diminishes the formation of liquid yield, the residence time of the pyrolysis vapors at high temperatures should be limited. The effect of this parameter on the bio-oil production has been studied by several authors, showing an increase in the liquid yield produced during the pyrolysis of sewage sludge when decreasing the residence time [24, 25].

In this work, a novel measurement technique is employed to analyze the evolution of the pyrolysis process of sewage sludge in a lab-scale bed reactor. The reactor was installed over a precision scale capable of measuring the mass released by the sewage sludge sample during its pyrolysis process, moving freely inside the reactor. This original measurement technique permits the study of the pyrolysis process to be focused on the solid fuel instead of analyzing only the liquid and/or the gas produced. The measurement obtained from the scale permitted the measurement of the evolution over time of the mass released by the sample for various operating conditions. The pyrolysis of sewage sludge was analyzed for six different Nitrogen velocities, from a velocity lower than the minimum fluidization velocity, corresponding to a fixed bed, to a velocity three times faster than the minimum fluidization velocity, which induces a bubbling fluidized bed. For each gas velocity, two different bed temperatures, 500 ºC and 600 ºC, in the range for which the liquid fuel production from pyrolysis is maximized, were tested. The pyrolysis time was obtained from the experimental

161 measurements, and a mathematical model based on a first order apparent
162 kinetics was proposed. The pyrolysis time estimated by the model was
163 compared to the experimental results obtaining a fairly good agreement.

164 **2. Theory**

165 Pyrolysis is a complex process in which a huge amount of chemical reactions
166 occur simultaneously or consecutively. The parallel reactions taking place are in
167 competition to each other and depend mainly on the pyrolysis conditions. A
168 simplified approach permits the variation of the sample mass with time, *dm/dt*,
169 to be determined as a function of the remaining volatile matter in the sample,
170 m_{vol}, and an apparent rate constant, *k*, for a determined reaction order, *n*, [23]
171 as:

$$\frac{dm}{dt} = -k \cdot m_{vol}{}^{n} \tag{1}$$

172 The mass of the sample, *m*, at each time, *t*, can be determined as the
173 summation of the volatile matter remaining in the sample, m_{vol}, and the solid
174 residue, m_{res}.

$$m = m_{vol} + m_{res} \tag{2}$$

175 Considering a first order reaction, *n* = 1, which is the simplest and most
176 generally used case, the integration of Eq. (1) reads:

$$m = m_{vol0} \cdot \exp\left(-k \cdot t\right) + m_{res} \tag{3}$$

177 where m_{vol0} is the initial mass of volatiles in the sample. Dividing Eq. (3) by the
178 initial mass of the sample, m_0, the evolution of the percentage of mass of the
179 sample, *X*, with time, *t*, can be estimated as a function of the initial percentage

of volatile content, X_{vol}, the percentage of solid residue, X_{res}, and the apparent rate constant, k. Notice that the percentage of solid residue is related to the initial volatile content of the sample as $X_{res} = 100 - X_{vol}$.

$$X = X_{vol} \cdot \exp(-k \cdot t) + X_{res} \quad (4)$$

3. Materials and methods

3.1. Experimental facility

The pyrolysis of the sewage sludge samples was carried out in a cylindrical lab-scale fluidized bed reactor, made of stainless steel, with an inner diameter, d_i, of 4.7 cm and a height, h, of 50 cm. The heat required to reach the reactor temperature for the pyrolysis was supplied by three electric resistors with a power of 500 W each one; one of them was located at the plenum and the other two over the distributor. A potentiometer was employed to control the thermal power released by the resistors. Nitrogen was used as the inert fluidization gas. The Nitrogen flowrate was supplied by a B50 bottle from Abelló Linde, containing Nitrogen 3.0 at a pressure of 200 bar. The Nitrogen flowrate was measured by a flowmeter PFM750-F01-F from SMC, with a measurement range from 1 to 50 l/min. The whole reactor, surrounded by the three resistors, rested on a precision scale PS 6000 R2 from RADWAG, capable of measuring up to 6 kg with a resolution of 0.01 g. A schematic of the experimental facility employed to conduct the pyrolysis experiments is shown in Fig. 1.

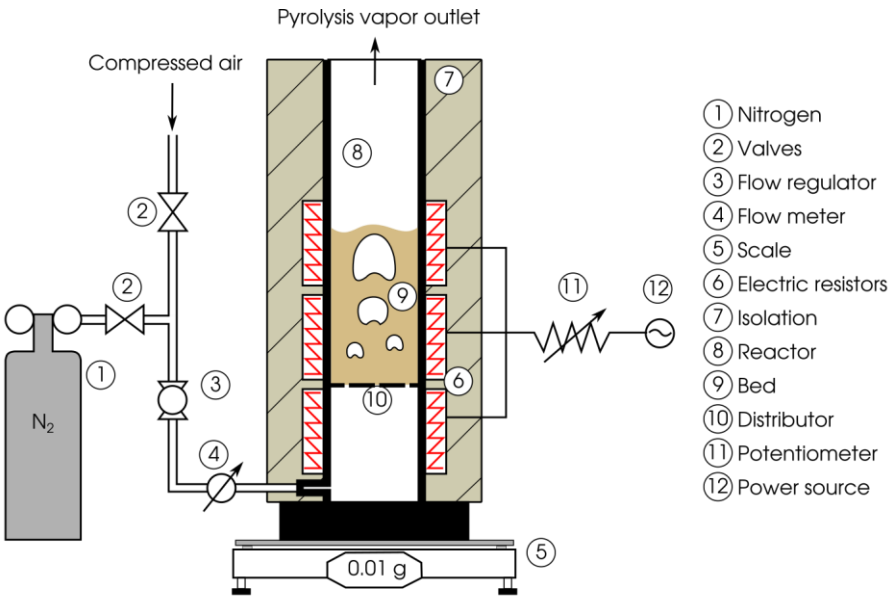

Fig. 1: Schematic of the experimental facility.

3.2. Bed material characterization

Silica sand was employed as bed material since it is known to be inert, not affecting the reaction rate during the thermochemical decomposition of biomass [26]. The silica sand particle diameter, d_{bm}, was in the range of 425 - 600 μm and the particle density, ρ_{bm}, was 2600 kg/m^3. A mass of 240 g of sand was used in each test to reach a fixed bed height, h_b, of 9.4 cm (bed aspect ratio h_b/d_i = 2), corresponding to a void fraction, ε, of 0.44.

The variation of the gas density, ρ_g, with temperature was considered to determine the minimum fluidization velocity, U_{mf}, as described in Sánchez-Prieto et al. [27]. The gas density at the reactor temperature was calculated considering the ideal gas law:

$$\rho_g = \rho_{g,amb} \frac{T_{amb}}{T} \quad (5)$$

where ρ_g is the Nitrogen density at temperature T and $\rho_{g,amb}$ is the Nitrogen density at the reference temperature T_{amb}. The reference temperature was

selected as T_{amb} = 300 K and the Nitrogen density at this temperature is $\rho_{g,amb}$ = 1.14 kg/m^3.

The minimum fluidization velocity can be estimated as a function of the reactor temperature using the correlation of Carman-Kozeny [28]:

$$U_{mf} = \frac{\left(\phi d_{bm}\right)^2 \left(\rho_{bm} - \rho_g\right) g}{180 \mu_g} \frac{\varepsilon^3}{1-\varepsilon} \tag{6}$$

where U_{mf} is the minimum fluidization velocity, ϕ is the sphericity of the dense phase particles, ε is the void fraction, g is the gravity acceleration, d_{bm} is the diameter of the bed material particles, ρ_{bm} is the density of the bed material particles, ρ_g is the density of Nitrogen at the reactor temperature, and μ_g is the dynamic viscosity of Nitrogen at the bed temperature. The variation of the dynamic viscosity of Nitrogen with the reactor temperature, T, can be determined by the potential law:

$$\mu_g = \mu_{g,amb} \left(\frac{T}{T_{amb}} \right)^{2/3} \tag{7}$$

where the dynamic viscosity of Nitrogen at the reference temperature (T_{amb} = 300 K) is $\mu_{g,amb}$ = 1.78·10^{-5} kg/(m·s).

4. Results and discussion

4.1. Minimum fluidization velocity

The minimum fluidization velocity of the silica sand particles was measured as a function of the bed temperature. Fig. 2 shows the experimental results of the minimum fluidization velocity, U_{mf}, together with the estimation from the Carman-Kozeny correlation (Eq. 6), as a function of the reactor temperature, T.

An average particle diameter of silica sand of d_{bm} = 512.5 μm and a sphericity of ϕ = 0.8 were selected for the Carman-Kozeny correlation. As can be seen in Fig. 2, the estimation of the Carman-Kozeny correlation properly describes the variation of the minimum fluidization velocity measured experimentally.

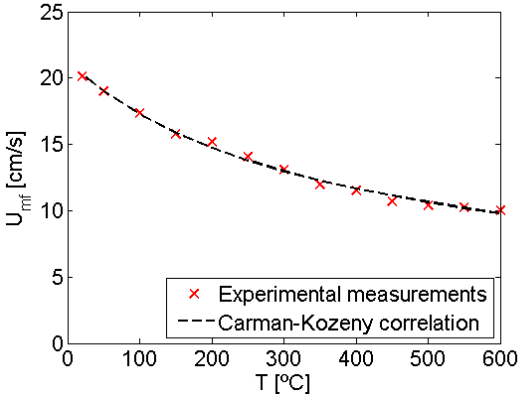

Fig. 2: Variation of the minimum fluidization velocity with the reactor temperature.

4.2. Sewage sludge characterization

The sewage sludge samples employed in this work were produced by the municipal sewage treatment plant of Loeches (Madrid, Spain) in February 2016. The sludge was taken after a pre-drying process at 80 ºC in a fluidized bed in the sewage treatment plant. Proximate and ultimate analyses were performed to characterize the samples. The former test was conducted in a TGA Q500 from TA Instruments, where the moisture, ash, volatile matter, and fixed carbon contents of the sample were determined.

The ultimate analysis of the sample was carried out in a LECO TruSpec CHN analyzer, where the Carbon and Hydrogen contents of the sample were measured using an infrared absorption detector for the exhaust gases obtained from the complete combustion of the sample carried out in pure Oxygen. The Nitrogen content is determined conducting the exhaust gases through a thermal

253 conductivity cell. The results of the proximate and ultimate analyses of the
254 sewage sludge samples are included in Table 1. Further details of the
255 characterization of the sewage sludge samples can be found in Soria-Verdugo
256 et al. [29]. The values obtained for the characterization of the sewage sludge
257 are similar to those obtained by different authors, such as [30-33].

258 Table.1: Results obtained from the proximate and ultimate analyses of the
259 sewage sludge (d: dry basis, daf: dry-ash-free basis, * obtained by difference).

Proximate analysis	
Volatile matter [% d]	57.11
Fixed carbon* [% d]	34.66
Ash [% d]	8.23
Elemental analysis	
C [% daf]	56.46
H [% daf]	7.91
N [% daf]	8.42
O* [% daf]	27.21

260 Prior to the pyrolysis experiments in the reactor, the sewage sludge samples
261 were sieved under a particle size d_p < 3 mm and dried at 105 °C in a universal
262 oven UFE 500 from Memmert for 5 hours, after which no mass variation of the
263 sample was detected. The pyrolysis of this sewage sludge under linear,
264 parabolic and exponential temperature increases in a thermogravimetric
265 analyzer (TGA) was studied in detail in a previous work [29].

266 **4.3. Pyrolysis experimental measurements**

267 The sewage sludge pyrolysis experiments consisted of recording the mass
268 signal measured by the scale while the pyrolysis process of the sewage sludge
269 sample was taking place inside the reactor. Therefore, the mass released
270 during the pyrolysis of the sampled could be determined. First, the reactor, filled
271 with the sand particles that conformed the bed, was heated by the resistors to

272 the desired reactor temperature, *T*, while an air flowrate was used as fluidizing
273 agent. Once the reactor temperature of the test was reached, the fluidizing gas
274 was switched to Nitrogen, and the flowrate was adjusted. When the operating
275 conditions of the bed, i.e. reactor temperature and Nitrogen flowrate, were
276 selected, the scale, in which the reactor rested, was tared and a batch of
277 around 10 g of dry sewage sludge particles was introduced through the top of
278 the reactor. Each experimental measurement was replicated to test the
279 reproducibility of the experimental procedure, obtaining deviations lower than
280 5%.

281 The mass signal measured by the scale during the pyrolysis of the sewage
282 sludge registered the vibration induced by the ascension of bubbles when the
283 bed was fluidized. Therefore, the mass signals measured in all cases were
284 filtered using a moving average. Further details of the filtration of the mass
285 signals can be found in a previous work [34]. The filtered signals were proved to
286 follow the average behavior of the raw signal measured by the scale in all
287 cases.

288 Different operating conditions were tested, varying both the reactor temperature
289 and the fluidizing gas velocity. The reactor temperatures analyzed in our work
290 are 500 and 600 ºC, temperatures for which the production of liquid fuel from
291 the condensation of the sewage sludge pyrolysis vapors is optimal. A
292 thermogravimetric analysis of the pyrolysis of the same sewage sludge studied
293 in this work showed that most of the mass released by the samples during the
294 pyrolysis occurs for temperatures below 500 ºC [29]. Concerning the velocity of
295 the fluidizing gas (Nitrogen) during the pyrolysis process, 6 different values
296 were tested for each reactor temperature, U/U_{mf} = 0.8, 1, 1.5, 2, 2.5, 3, from a

297 velocity lower than U_{mf}, corresponding to a fixed bed reactor, to 3 times U_{mf},
298 which induces a bubbling fluidized regime in the reactor. Gas velocities higher
299 than $3U_{mf}$ may produce large bubbles in the bed compared to the reactor
300 diameter, leading to a slugging regime, which is not the focus of this work.

301 **4.4. Evolution of the sewage sludge mass during the pyrolysis process**

302 The evolution with time of the mass of the sewage sludge sample during the
303 pyrolysis, measured by the scale, was filtered and divided by the initial mass of
304 the sample, m_0, to obtain the percentage of mass remaining, X. The variation of
305 X with time during the pyrolysis of sewage sludge for each gas velocity
306 analyzed are plotted in Fig. 3 a) for a reactor temperature of 500 ºC and in Fig.
307 3 b) for a bed temperature of 600 ºC. The pyrolysis process is accelerated when
308 increasing the fluidizing gas velocity for the two reactor temperatures tested.
309 This fact can be attributed to the increase of the heating rate of the sewage
310 sludge particles [9, 35] caused by the higher axial fuel mixing obtained when the
311 fluidizing gas velocity is increased [14, 15]. Comparing the experimental
312 measurements obtained for both reactor temperatures, a slight effect of the
313 temperature can be observed, accelerating scarcely the pyrolysis process when
314 increasing the reactor temperature from 500 ºC to 600 ºC. Nevertheless, the
315 effect of the reactor temperature on the pyrolysis process is lower in
316 comparison with the significant effect of increasing the fluidization velocity.

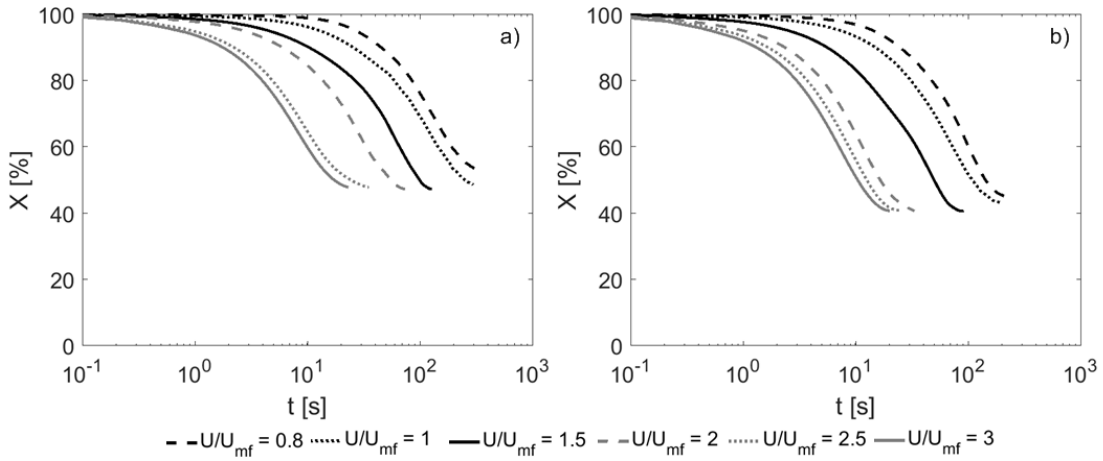

Fig. 3: Evolution with time of the percentage of mass of the sewage sludge sample remaining in the reactor for a bed temperature of a) 500 ºC and b) 600 ºC.

To facilitate the analysis of the effect of the reactor temperature on the pyrolysis process, the derivative of the percentage of mass remaining in the reactor is plotted as a function of time in Fig. 4. The derivative of the percentage of mass is clearly increased for both reactor temperatures when increasing the fluidization velocity, accelerating the pyrolysis of the samples as stated above. Comparing the results plotted in Fig. 4 a) for a reactor temperature of 500 ºC with those in Fig. 4 b) obtained for a bed temperature of 600 ºC, the increase of the derivative of *X* with temperature can be observed. Therefore, the pyrolysis reaction of sewage sludge can be accelerated by increasing the gas velocity and/or the reactor temperature.

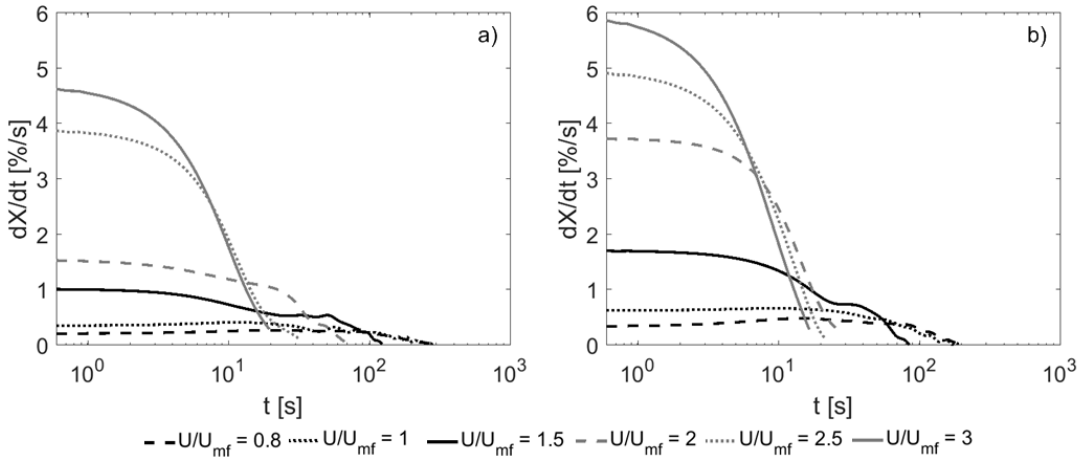

Fig. 4: Variation with time of the derivative of the percentage of mass of the sewage sludge sample remaining in the reactor for a bed temperature of a) 500 ºC and b) 600 ºC.

The percentage of mass remaining after the pyrolysis process, X_{res}, can be determined as the percentage of mass at the end of the tests shown in Fig. 3. It can be observed in Fig. 3 that this percentage of mass remaining, X_{res}, depends on the operating conditions. To analyze the effect of both the reactor temperature and the Nitrogen velocity on the mass remaining after the pyrolysis, X_{res}, Fig. 5 shows the percentage of mass of volatiles released by the sample during the complete pyrolysis process, X_{vol}, defined as X_{vol} = 100 - X_{res}. Thermogravimetric analysis (TGA) tests of the pyrolysis of sewage sludge samples were also carried out for comparison to the pyrolysis tests in the reactor. The TGA tests were conducted in the TGA Q500 from TA Instruments and consisted of measuring the evolution of an initial mass of 10 mg of sewage sludge in a Nitrogen atmosphere at temperatures of 500 ºC and 600 ºC. The percentage of volatile matter released by the sewage sludge during the pyrolysis in the TGA is also included in Fig. 5 as dotted (T = 500 ºC) and dashed (T = 600 ºC) lines for comparison, although the Nitrogen flowrate for all the TGA tests was maintained constant at 60 ml/min.

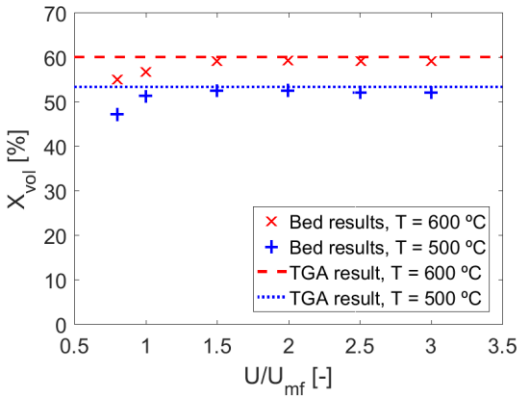

Fig. 5: Total volatile matter released by the sewage sludge sample.

The percentage of volatile matter released by the samples during the pyrolysis process in the reactor is very similar to that obtained in the TGA, provided that the Nitrogen velocity is sufficient to induce a proper fluidization of the bed ($U/U_{mf} \geq 1.5$). However, when the pyrolysis occurs in a fixed bed ($U/U_{mf} = 0.8$) or in a bed at minimum fluidization velocity ($U/U_{mf} = 1$), the value of X_{vol} obtained in the reactor is lower than that of the TGA. This can be attributed to heat transfer effects inside the sample when no bubbles are present in the bed ($U/U_{mf} \leq 1$) and the fuel particles accumulate on the bed surface after being introduced in a batch through the bed top, and thus the low conduction of heat inside this accumulation of fuel particles in the surface is important. When the gas velocity is increased above the minimum fluidization velocity ($U/U_{mf} > 1$), bubbles appear in the bed and induce the motion of fuel particles, breaking the typical accumulation of fuel found in fixed beds, and enhancing the axial dispersion of fuel inside the bed [14, 15]. Therefore, in the case of fluidized beds, the fuel particles are separated from each other due to the higher dispersion of fuel induced by the presence of bubbles, hence the effect of heat transfer inside the sample is reduced, and the heating rate is increased.

370 The values of the percentage of volatile matter released during the pyrolysis of
371 sewage sludge, X_{vol}, shown in Fig. 5 are in accordance with those reported by
372 different authors in the literature. Regarding the pyrolysis of sewage slugde in a
373 fixed bed, Wang et al. [1] obtained values of X_{vol} = 50.9% and X_{vol} = 55% for
374 reactor temperatures of 500 ºC and 600 ºC respectively, whereas Atienza-
375 Martínez et al. [36] reached X_{vol} = 51% for a bed temperature of 530 ºC. Despite
376 the great heterogeneity in the composition of sewage sludge, these values are
377 quite close to those obtained in our work, X_{vol} = 47.2% for T = 500 ºC and X_{vol} =
378 55.1% for T = 600 ºC. Concerning the pyrolysis of sewage sludge in a fluidized
379 bed, Shen and Zhang [25] obtained percentages of volatile matter of X_{vol} =
380 55.2% and X_{vol} = 57.4% for fluidized bed temperatures of 500 ºC and 600 ºC,
381 respectively, which are comparable to those obtained in this work X_{vol} = 53.4%
382 (T = 500 ºC) and X_{vol} = 60.1% (T = 600 ºC) in the TGA tests. Furthermore,
383 several authors informed of a reduction of the solid residue produced during the
384 pyrolysis of biomass for higher heating rates [9, 23, 37] and pyrolysis
385 temperatures [6, 16, 19, 20, 25].

386 **4.5. Pyrolysis time**

387 The effect of the different volatile matter released for each operating condition
388 can be removed by re-scaling the evolution of the percentage of sewage sludge
389 mass remaining in the reactor, X, shown in Fig. 3, to calculate the reacted
390 fraction, V/V^*. The reacted fraction, V/V^*, is defined as the ratio of the volatile
391 matter released at a determined time to the total volatile matter released after
392 the complete pyrolysis process, thus V/V^* = 0% at the beginning of the pyrolysis
393 process and V/V^* = 100% when the process ends. The results obtained for the
394 reacted fraction, V/V*, are shown in Fig. 6, where a very similar shape of the

curves obtained for the different gas velocities and reactor temperatures can be observed. The increase of either the gas velocity or the bed temperature produces a displacement of the curves to shorter times, reducing the time needed for the pyrolysis of the sample.

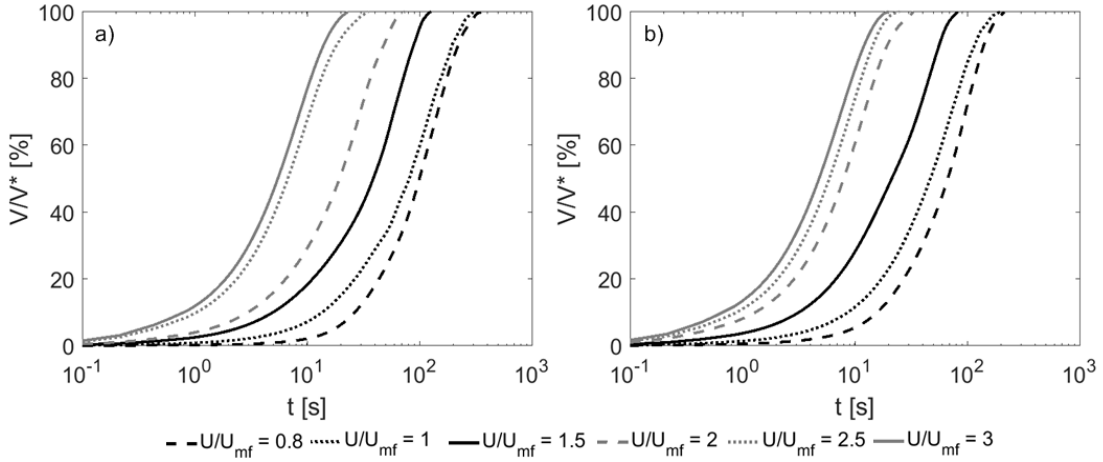

Fig. 6: Evolution of the reacted fraction of sewage sludge with time for reactor temperatures of a) 500 ºC and b) 600 ºC.

The pyrolysis time, t_{pyr}, can be calculated as the time needed to reach a determined value of the reacted fraction. In this work, a value of V/V^* = 95% is selected to determine the pyrolysis time. Fig. 7 shows the pyrolysis time of sewage sludge as a function of the Nitrogen velocity for the two different reactor temperatures studied. A substantial reduction of the pyrolysis time can be obtained by raising the fluidization velocity. The reduction of the pyrolysis time between a fixed or minimum fluidization bed ($U/U_{mf} \leq 1$) and a bubbling fluidized bed reactor ($U/U_{mf} \geq 1.5$) is significant, due to the higher heating rate characteristic of fluidized beds [24]. A clear reduction of the pyrolysis time with the reactor temperature can be also observed for low gas velocities ($U/U_{mf} <$ 2.5). However, these differences are negligible when increasing the Nitrogen velocity ($U/U_{mf} \geq 2.5$).

The reduction of the pyrolysis time produced by fluidized bed reactors is of central importance for industrial reactors since a lower pyrolysis time, i.e. faster pyrolysis reaction rate, permits the increase of the fuel feeding rate and, thus, the production of liquid fuel from the condensation of the pyrolysis vapors is enhanced. Furthermore, a higher fluidizing gas velocity reduces the pyrolysis vapors residence time in the reactor, promoting a higher content of condensable gases in the pyrolysis vapors, which further improves the production of liquid fuel from the pyrolysis of the sample [9, 17, 25].

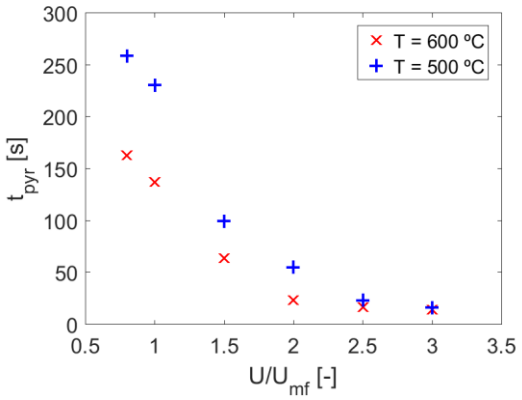

Fig. 7: Pyrolysis time of sewage sludge for reactor temperatures of a) 500 ºC and b) 600 ºC.

4.6. Modelling of the pyrolysis process of sewage sludge

In this section, a mathematical procedure to estimate the pyrolysis time of sewage sludge as a function of the operating conditions of the reactor is presented. The procedure is based on determining the apparent rate constant, *k*, for the different gas velocities and reactor temperatures studied experimentally. The apparent rate constant, *k*, can be determined by fitting the experimental curves of the evolution of the percentage of mass of the sample, *X*, with time, shown in Fig. 3, to an exponential decay function in the form of Eq. (4). The fitting of the experimental curves *X* – *t* was carried out only for Nitrogen

velocities high enough to properly fluidize the bed, i.e. $U/U_{mf} \geq 1.5$, causing a negligible effect of heat transfer inside the sample. For the pyrolysis tests of high gas velocities ($U/U_{mf} \geq 1.5$), the percentage of volatile matter released by the sewage sludge can be considered to be an exclusive function of temperature, being X_{vol} = 53.4% for a reactor temperature of 500 ºC and X_{vol} = 60.1% for a bed temperature of 600 ºC (see Fig. 5). Therefore, the only free parameter on the fitting of the evolution of X with time to Eq. (4) is the apparent rate constant, k. The values obtained for the apparent rate constant, k, for each operating condition are included in Table 2, together with the determination coefficient, R^2, of the fitting. As can be observed in Table 2, the determination coefficient, R^2, is higher than 0.98 in all the cases analyzed, thus the experimental data of the variation of the percentage of mass of sewage sludge during the pyrolysis in the bubbling fluidized bed reactor can be said to follow a first order apparent kinetics.

Table 2: Values of the apparent rate constant and determination coefficient of the fitting for different gas velocities and reactor temperatures.

	T = 500 ºC		T = 600 ºC	
U/U_{mf} [-]	k [min^{-1}]	R^2 [-]	k [min^{-1}]	R^2 [-]
1.5	1.25	0.981	2.07	0.986
2	2.43	0.983	5.88	0.985
2.5	6.48	0.996	7.89	0.984
3	8.18	0.991	9.61	0.987

The values obtained for the apparent rate constant, included in Table 2, are depicted in Fig. 8 as a function of the dimensionless gas velocity, U/U_{mf}, for both reactor temperatures, along with a linear fitting of the data.

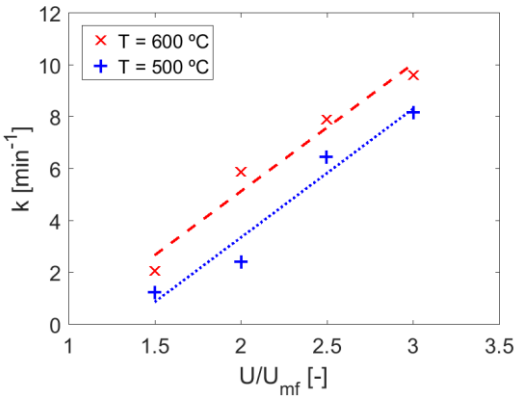

Fig. 8: Apparent rate constant obtained from the fitting as a function of the gas velocity.

The variation of the apparent rate constant, k, with the dimensionless gas velocity, U/U_{mf}, was fitted to a linear equation, obtaining the slopes and intercepts presented in Eq. (8) and Eq. (9) for T = 500 ºC and T = 600 ºC, respectively. The increase of the apparent rate constant with the gas velocity is similar for the two reactor temperatures analyzed, as can be observed from the similar values of the slopes in Eqs. (8) and (9). The reactor temperature affects only the intercept of the linear fitting of the apparent rate constant with the dimensionless gas velocity.

$$k_{500} = 4.97\left(U / U_{mf}\right) - 6.59 \tag{8}$$

$$k_{600} = 4.92\left(U / U_{mf}\right) - 4.71 \tag{9}$$

The pyrolysis time can be estimated, t_{mod}, using the first order kinetic model described in section 2, as an only function of the apparent rate constant obtained for each bed temperature and gas velocity. Eqs. (8) and (9) can be used to estimate the value of the apparent rate constant for the pyrolysis of sewage sludge in a bubbling fluidized bed as a function of the gas velocity, for reactor temperatures of 500 ºC and 600 ºC, respectively. The estimated values

of the apparent reaction velocities, k_{500} and k_{600}, can be introduced in Eq. (4) to estimate numerically the evolution of the percentage of mass of the sewage sludge sample, X, with time during the pyrolysis process. This numerical estimation of the evolution of X with time can be rescaled to obtain a numerical reacted fraction, V/V^*, that can be employed to calculate the estimated pyrolysis time, t_{mod}, as the time for which the numerical reacted fraction reaches 95%. The results obtained for the estimation of the pyrolysis time, t_{mod}, are presented in Table 3 together with the experimental results, t_{pyr}, for comparison. The relative error, ε_t, between the estimated and the experimental pyrolysis time is also included in Table 3 for each operating condition of the fluidized bed reactor. The results presented in Table 3 show a good agreement between the prediction of the pyrolysis time by the model and the experimental results, obtaining relative errors around 10%.

Table 3: Comparison between the estimated and experimental pyrolysis times for different gas velocities and reactor temperatures.

	T = 500 ºC			T = 600 ºC		
U/U_{mf} [-]	t_{pyr} [s]	t_{mod} [s]	ε_t [%]	t_{pyr} [s]	t_{mod} [s]	ε_t [%]
1.5	99.9	111.2	11.3	63.7	60.9	4.4
2	55.6	49	11.9	23.7	26.3	11
2.5	23.4	25.8	10.2	17	19.1	12.3
3	16.8	17.5	4.2	14.3	14.9	4.3

5. Conclusions

The pyrolysis process of sewage sludge was studied experimentally in a bed reactor, analyzing the evolution of the sample mass with time for different reactor temperatures and gas velocities. For high gas velocities, corresponding to a bubbling fluidized bed regime ($1.5 \leq U/U_{mf} \leq 3$), the pyrolysis process was accelerated due to the higher heating rate of fuel particles in fluidized beds in

comparison to fixed bed reactors. The pyrolysis process occurs faster also for higher reactor temperatures, although the effect of the bed temperature is slight compared to that of the gas velocity. The percentage of volatile matter released by the sewage sludge sample during the pyrolysis in a bubbling fluidized bed reactor was around 53.4% for a bed temperature of 500 ºC and 60.1% for a temperature of 600 ºC. These results are in accordance with the literature, and very similar to those obtained from a thermogravimetric analysis of the samples. The amount of volatile matter released by the sewage sludge is slightly lower when the pyrolysis process is carried out in a fixed bed reactor.

The pyrolysis time was determined experimentally from the evolution of the reacted fraction of the sewage sludge, showing and important diminution when the gas velocity increases due to the larger heating rates characteristic of bubbling fluidized beds. The effect of the reactor temperature is significant for low gas velocities, whereas for high gas velocities the influence of the bed temperature is negligible. A mathematical procedure, based on a first order apparent chemical kinetics and capable of predicting the evolution of the complex pyrolysis process, was proposed. The apparent pyrolysis rate constant was obtained from a fitting of the experimental data to the first order kinetics equation. The apparent rate constant showed a linear increased with the gas velocity, maintaining a constant slope for the two different bed temperatures studied. Finally, the mathematical model proposed was employed to estimate the pyrolysis time for each operating condition, showing a good agreement with the experimental pyrolysis time, obtaining deviations of around 10% for all the operating conditions analyzed.

Acknowlegments

The authors gratefully acknowledge the financial support provided by Fundación Iberdrola under the program “Programa de Ayudas a la Investigación en Energía y Medioambiente”.

References

[1] Wang X., Deng S., Tan H., Adeosun A., Vujanovic M., Yang F., Duic N. 2016. Synergetic effect of sewage sludge and biomass co-pyrolysis: A combined study in thermogravimetric analyzer and a fixed bed reactor. Energy Conversion and Management 118, 399-405.

[2] Fonts I., Gea G., Azuara M., Ábrego J., Arauzo J. 2012. Sewage sludge pyrolysis for liquid production: A review. Renewable and Sustainable Energy Reviews 16, 2781-2805.

[3] Kaminsky W., Kummer A.B. 1989. Fluidized bed pyrolysis of digested sewage sludge. Journal of Analytical and Applied Pyrolysis 16, 27-35.

[4] Fytili D., Zabaniotou A. 2008. Utilization of sewage sludge in EU application of old and new methods – A review. Renewable and Sustainable Energy Reviews 12,116-40.

[5] Sun Y., Jin B, Wu W., Zuo W., Zhang Y., Zhang Y., Huang Y. 2015. Effects of temperature and composite alumina on pyrolysis of sewage sludge. Journal of Environmental Sciences 30, 1-8.

[6] Yan Q., Toghiani H., Yu F., Cai Z., Zhang J. 2011. Effects of pyrolysis conditions on yield of bio-chars from pine chips. Forest Products Journal 61, 367-371.

538 [7] Bridgwater A.V. 2012. Review of fast pyrolysis of biomass and product
539 upgrading. Biomass and Bioenergy 38, 68-94.

540 [8] Bridgwater A.V., Peacoke G.V.C. 2000. Fast pyrolysis process for biomass.
541 Renewable and Sustainable Energy Reviews 4, 1-73.

542 [9] Bridgwater A.V., Meier D., Radlein D. 1999. An overview of fast pyrolysis of
543 biomass. Organic Geochemistry 30, 1479-1493.

544 [10] Leckner B. 2016. Developments in fluidized bed conversion of solid fuels.
545 Thermal Science 20, S1-S18.

546 [11] Leckner B. 1998. Fluidized bed combustion: Mixing and pollutant limitation.
547 Progress in Energy Combustion Science 24, 31-61.

548 [12] Soria-Verdugo A., García-Hernando N., Almendros-Ibáñez J.A., García-
549 Hernando U. 2011. Motion of a large object in a bubbling fluidized bed with a
550 rotating distributor. Chemical Engineering and Processing 50, 859-868.

551 [13] Soria-Verdugo A., García-Gutiérrez L.M., Sánchez-Delgado S., Ruiz-Rivas
552 U. 2011. Circulation of an object immersed in a bubbling fluidized bed.
553 Chemical Engineering Science 66, 78-87.

554 [14] Soria-Verdugo A., García-Gutiérrez L.M., García-Hernando N., Ruiz-Rivas
555 U. 2011. Buoyancy effects on objects moving in a bubbling fluidized bed.
556 Chemical Engineering Science 66, 2833-2841.

557 [15] Lundberg L., Soria-Verdugo A., Pallarès D., Johansson R, Thunman H.
558 2016. The role of fuel mixing on char conversion in a fluidized bed. Powder
559 Technology, In Press.

560 [16] Park E.S., Kang B.S, Kim J.S. 2008. Recovery of oils with high caloric
561 value and low contaminant content by pyrolysis of digested and dried sewage
562 sludge containing polymer flocculants. Energy and Fuels 22, 1335-1340.

563 [17] Park H.J., Heo H.S., Park Y.K., Yim J.H., Jeon J.K., Park J., Ryu C., Kim
564 S.S., 2010. Clean bio-oil production from fast pyrolysis of sewage sludge:
565 Effects of reaction conditions and metal oxide catalysts. Bioresource
566 Technology 101, 83-85.

567 [18] Arazo R.O., Genuino D.A.D., de Luna M.D.G., Capareda S.C. 2017. Bio-oil
568 production from dry sewage sludge by fast pyrolysis in an electrically-heated
569 fluidized bed reactor. Sustainable Environmental Research 27, 7-14.

570 [19] Jaramillo-Arango A., Fonts I., Chejne F., Arauzo J. 2016. Product
571 compositions from sewage sludge pyrolysis in a fluidized bed and correlations
572 with temperature. Journal of Analytical and Applied Pyrolysis 121, 287-296.

573 [20] Alvarez J., Amutio M., Lopez G., Barbarias I., Bilbao J., Olazar M. 2015.
574 Sewage sludge valorization by flash pyrolysis in a conical spouted bed reactor.
575 Chemical Engineering Journal 273, 173-183.

576 [21] Fonts I., Juan A., Gea G., Murillo M.B., Sánchez J.L. 2008. Sewage sludge
577 pyrolysis in fluidized bed, 1: Influence of operational conditions on the product
578 distribution. Industrial & Engineering Chemistry Research 47, 5376-5385.

579 [22] Sun Y., Jin B.S., Huang Y.J., Zuo W., Jia J.Q., Wang Y.Y. 2013.
580 Distribution and characteristics of products from pyrolysis of sewage sludge.
581 Advanced Materials Research 726, 2885-2893.

582 [23] Reschmeier R., Roveda D., Müller D., Karl J. 2014. Pyrolysis kinetics of
583 wood pellets in fluidized beds. Journal of Analytical and Applied Pyrolysis 108,
584 117-129.

585 [24] Piskorz J., Scott D.S., Westerberg I.B. 1986. Flash Pyrolysis of Sewage
586 Sludge. Industrial & Engineering Chemistry Process Design and Development
587 25, 265-270.

588 [25] Shen L., Zhang D.K., 2003. An experimental study of oil recovery from
589 sewage sludge by low-temperature pyrolysis in a fluidized-bed. Fuel 82, 465-
590 472.

591 [26] Koppatz M., Pfeifer C., Hofbauer H. 2011. Comparison of the performance
592 behavior of silica sand and olivine in a dual fluidized bed reactor system for
593 steam gasification of biomass as a pilot plant scale. Chemical Engineering
594 Journal 175, 468-483.

595 [27] Sánchez-Prieto J., Soria-Verdugo A., Briongos J.V., Santana D. 2014. The
596 effect of temperature on the distributor design in bubbling fluidized beds.
597 Powder Technology 261, 176–184.

598 [28] Carman P.C. 1937. Fluid flow through granular beds. Transactions of the
599 Institute of Chemical Engineers 15, 150-166.

600 [29] Soria-Verdugo A., Goos E., Morato-Godino A., Garcia-Hernando N., Riedel
601 U. 2017. Pyrolysis of biofuels of the future: Sewage sludge and microalgae –
602 Thermogravimetric analysis and modelling of the pyrolysis under different
603 temperature conditions. Energy Conversion and Management 138, 261-272.

604 [30] Scott S.A., Dennis J.S., Davidson J.F., Hayhurst A.N. 2006.
605 Thermogravimetric measurements of the kinetics of pyrolysis of dried sewage
606 sludge. Fuel 85, 1248-53.

607 [31] Soria-Verdugo A., Garcia-Hernando N., Garcia-Gutierrez L.M., Ruiz-Rivas
608 U. 2013. Analysis of biomass and sewage sludge devolatilization using the
609 distributed activation energy model. Energy Conversion and Management 65,
610 239-244.

611 [32] Jayaraman K., Gökalp I. 2015. Pyrolysis, combustion and gasification
612 characteristics of miscanthus and sewage sludge. Energy Conversion and
613 Management 89, 83-91.

614 [33] Liu G., Song H., Wua J. 2015. Thermogravimetric study and kinetic
615 analysis of dried industrial sludge pyrolysis. Waste Management 41, 128-133.

616 [34] Soria-Verdugo A., Morato-Godino A., Garcia-Gutierrez L.M., Garcia-
617 Hernando N. 2017. Pyrolysis of sewage sludge in a bubbling fluidized bed:
618 Determination of the reaction rate. 12th International Conference on Fluidized
619 Bed Technology (CFB 12). Krakow, Poland.

620 [35] Scott D.S., Piskorz J. 1984. The continuous flash pyrolysis of biomass.
621 Canadian Journal of Chemical Engineering 62, 404-412.

622 [36] Atienza-Martínez M., Fonts I., Lázaro L., Ceamanos J., Gea G. 2015. Fast
623 pyrolysis of torrefied sewage sludge in a fluidized bed reactor. Chemical
624 Engineering Journal 259, 467-480.

625 [37] Damartzis T.H., Vamvuka D., Sfakiotakis S., Zabaniotou A. 2011. Thermal
626 degradation studies and kinetic modeling of cardoon (*Cynara cardunculus*)

627 pyrolysis using thermogravimetric analysis (TGA). Bioresource Technology 102,
628 6230-6238.

List of Figures

647 **List of Tables**